Journal of Thermal Analysis and Calorimetry, Vol. 88 (2007) 2, 477–482

# THERMOGRAVIMETRY/MASS SPECTROMETRY ANALYSIS OF ENERGY CROPS

*Erika Mészáros*[1*], *Emma Jakab*[1], *G. Várhegyi*[1] *and P. Tóvári*[2]

[1]Institute of Materials and Environmental Chemistry, Chemical Research Center, Hungarian Academy of Sciences
1525 Budapest, P.O. Box 17, Hungary
[2]Hungarian Institute of Agricultural Engineering, Gödöllő, Hungary

The aim of this work was to study the thermal decomposition of different plant species obtained from energy plantations. Thermogravimetry/mass spectrometry (TG/MS) experiments have been performed with two herbaceous crops (*Miscanthus sinensis,* pelletized energy grass) and two wood samples (willow, water locust) in inert and oxidative atmospheres. Owing to the large number of data obtained in the experiments, a chemometric tool, principal component analysis (PCA) has been used to help the interpretation of the results. It has been found that the thermal decomposition of the studied wood species is similar, whereas that of the studied herbaceous samples exhibits significant differences. PCA has been found to be useful for finding correlations between the various experimental data.

***Keywords:*** *biomass, energy grass, Miscanthus sinensis, principal component analysis (PCA), thermogravimetry/mass spectrometry, water locust, willow*

## Introduction

Biomass is a rather important and promising renewable energy and raw material source. Plant materials can be utilized with thermochemical or biochemical conversion processes [1, 2]. Combustion to produce energy is one of the most obvious and widespread applications of plant materials. However, for the optimal utilization of biomass materials as a source of energy, a thorough knowledge and understanding of their thermal behavior is necessary.

During the past decades, extensive research has been carried out in the field of biomass pyrolysis. The thermal decomposition, and the composition of different species have been studied, the calorific values of the samples have been determined [3–7]. Lately, special fast growing species grown on energy plantations [8–11] have been in the focus of interest besides wastes of plant origin [12, 13].

Several authors have used different mathematical tools for a better interpretation of the experimental results. Various reaction kinetic models have been worked out for the description of the decomposition of plant species. In addition, chemometrics is also becoming more important in the field of thermal analysis [11, 14–19].

The aim of the present work was to study four different plant species, which were improved for energy production. Some papers have already been published about *Miscanthus sinensis* [3] and willow [11, 20], however, the place of origin and the age of the plants can have a great effect on the composition [6, 21], consequently, on the thermal behavior of the biomass samples. Two of these species (pelletized energy grass and water locust) are novel energy plants, which have not been investigated before.

## Experimental

Willow (*Salix alba*), water locust (*Amorpha fructicosa*), *Miscanthus sinensis* (Chinese silvergrass) and energy grass (*Agropyron*) samples from an energy plantation were studied in this work. The wood samples and *Miscanthus sinensis* were small chips obtained from young plants harvested in February, 2005. The energy grass was pelletized. Prior to analysis all samples have been dried at room temperature and milled to pass 120 μm sieves. The amount of Klason-lignin has been determined according to the ASTM E 1721-01 standard method. The calorific values of the samples have been measured according to the CEN/TS 14918 standard method with an IKA C2000 calorimeter. The ash content of the samples was determined according to the CEN/TS 14775 procedure supplemented by an additional heating of the ash at 850°C for 120 min. The above characteristics of the samples are listed in Table 1.

The TG/MS system used in this work was built from a Perkin-Elmer TGS-2 thermobalance and a Hiden Hal quadrupole mass spectrometer. The measurements have been carried out in argon and argon:oxygen=79:21 gases. Prior to the experiments, the apparatus was purged with the carrier gas for

* Author for correspondence: m_erika@chemres.hu

1388–6150/$20.00
© 2007 Akadémiai Kiadó, Budapest
Akadémiai Kiadó, Budapest, Hungary
Springer, Dordrecht, The Netherlands

**Table 1** Characteristics of the studied samples (on dry basis)

| Sample | | Klason-lignin*/ mass/mass% | Ash/ mass/mass% | Calorific value/ MJ $kg^{-1}$ |
|---|---|---|---|---|
| Name | Abbreviation | | | |
| Willow (*Salix alba*) | *SA* | 26.5 | 1.4 | 17.3 |
| Water locust (*Amorpha fructicosa*) | *AF* | 17.1 | 1.2 | 16.9 |
| Energy grass (*Agropyron*) | *AP* | 21.8 | 5.6 | 16.1 |
| *Miscanthus sinensis* (Chinese silvergrass) | *MS* | 21.0 | 1.8 | 17.0 |

*The determination of the amount of acid-insoluble lignin (Klason-lignin) was performed on the samples without preliminary extraction. Hence the data listed in this table give the total amount of lignins and phenolic polymers which are structurally related to condensed tannins [22]

45 min. In inert atmosphere 4 mg samples were heated from 20 to 900°C at a rate of 20°C $min^{-1}$, whereas in the presence of oxygen 0.4 mg sample sizes were used at a heating rate of 10°C $min^{-1}$ to avoid heat and mass transfer problems. For the 0.4 mg sample size baseline correction was applied: the TG curve of the empty sample holder was subtracted. A portion of the volatiles formed as a result of thermal decomposition was led through a glass lined metal capillary transfer line kept at 300°C to the ion source of the mass spectrometer. The mass spectrometer was operated in the electron ionization mode with 70 eV energy. The ion intensities were normalized to the intensity of the $^{38}Ar$ isotope of the carrier gas to avoid errors resulting from a shift in the sensitivity of the mass spectrometer.

Principal component analysis (PCA) was carried out on two data sets. The first matrix consisted of data of Table 1 and characteristic TG and DTG data obtained in inert and oxidative atmosphere ($T_{hc.on,}$ onset of hemicellulose decomposition; $T_{cell.off}$, offset of cellulose decomposition; $T_{peak}$, DTG peak temperature; $DTG_{max}$, DTG peak maximum and char yield) determined as described previously [6, 20]. In the second step we have attempted to find correlation between the integrated intensities of the most important decomposition products, which are listed in Table 2.

## Results and discussion

*Results of the TG/MS experiments*

Figure 1 presents the TG and DTG curves of the studied samples in inert atmosphere. The results show that the thermal decomposition of the herbaceous species (energy grass, *AP* and *Miscanthus sinensis*, *MS*) starts at a lower temperature and proceeds at a higher rate than that of the wood species (willow, *SA* and water locust, *AF*). The carbonaceous residue of the energy grass is the highest, whereas that of the water locust is the lowest. The other two species give about the same amount of char. The comparison of the wood samples shows that the profiles of the DTG curves are similar, differences can only be observed in the height of the shoulder corresponding to hemicellulose decomposition (at about 320°C) and in the char yield. These differences can mainly be attributed to the different composition of the two wood samples (Table 1). The characteristic shoulder on the main DTG peak, which can be attributed to hemicellulose decomposition, can be observed for energy grass (at 280°C) as well. The cellulose and hemicellulose decomposition are more overlapped in the case of *Miscanthus sinensis* (*MS*), and a smaller shoulder can be seen on this curve at about 210°C, which can presumably be attributed to decomposition of extractable compounds.

The mass spectrometric curves of the evolved products give further information about the decomposition reactions. The main decomposition products of biomass materials are water, carbon monoxide and carbon dioxide, and smaller amounts of methane and hydrogen are also released from plant samples as it has been discussed extensively in previous studies [3, 11]. In addition, several organic volatiles (e.g. acids, ketones, aldehydes, furan derivatives, aromatic compounds) are formed in the slow pyrolysis process. In Figs 2a–f the mass spectrometric curves of the fragment ions of some decomposition products are shown. The *m/z* 16 ion corresponds to methane, which can be produced in different processes, as the broad, multiple peaks of Fig. 2a imply. It can be seen that methane formation from lignin (peak at about 420°C) is more pronounced for the *SA*, *AF* and *MS* samples, whereas a higher amount of methane is formed in the charring processes in the case of the *AP* sample (peak at 530°C). The smaller peak at 290°C on the MS curve of *Miscanthus sinensis* can be attributed to the decomposition of the extractable components.

Figure 2b shows the MS curve of an aliphatic fragment ion, $C_2H_2^+$. There is a marked similarity in the shape of these MS curves and the profile of the corresponding DTG curves. Hence, it can be concluded that the major decomposition processes contribute to the formation of this fragment ion. It is interesting to note the shoulder at about 470–510°C, which may also correspond to the decomposition of extractive constituents of plants. The smaller peak on the mass spectrometric curve of the *Miscanthus*

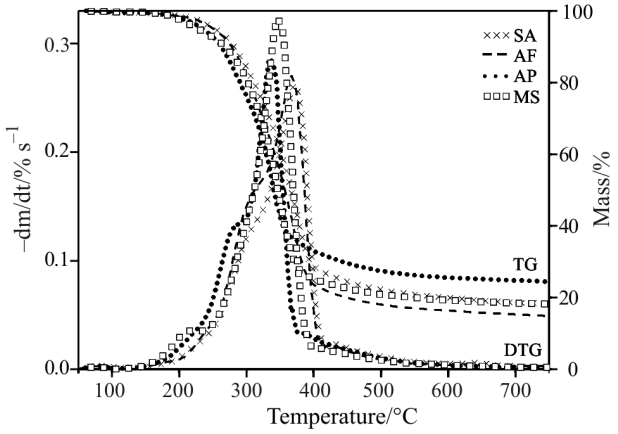


**Fig. 1** TG and DTG curves of the samples in inert atmosphere

*sinensis* sample at 220°C can also be attributed to the decomposition of extractive components.

The *m*/*z* 31 ion ($CH_3O^+$) (Fig. 2c) corresponds to the main fragment ion of hydroxyacetaldehyde and methanol. The former product is released in the thermal decomposition of cellulose, the latter one is produced as a result of the scission of lignin and hemicellulose sidegroups. The decomposition of hemicellulose and cellulose is clearly separated in the case of the wood samples (*SA* and *AF*) indicated by the distinct shoulders on the corresponding MS curves. However, the heights of these shoulders are considerably different for the two wood samples (similarly to the DTG curves, Fig. 1) reflecting that the relative amount of hemicelluloses is different in the two species. The $CH_3O^+$ ion is the most abundant from the *MS* sample, however, in this case the hemicellulose decomposition is not well separated from that of cellulose. The energy grass (*AP*) sample gives the smallest yield of this product.

The $COOH^+$ fragment ion (*m*/*z* 45) (Fig. 2d) is also released in the decomposition of polysaccharides. The amount of acids produced in the decomposition of cellulose and hemicellulose are comparable for the wood samples. A relatively lower acid yield can be observed from the energy grass sample (*AP*). The formation of acids from cellulose and hemicellulose is not separated in the case of the *Miscanthus sinensis* sample (*MS*). The thermal decomposition of extractives is indicated by the peak at 200°C.

**Fig. 2** Mass spectrometric curves of some characteristic fragment ions of biomass decomposition (argon atmosphere). Notation: ××× – willow (*Salix alba*); --- – water locust (*Amorpha fructicosa*); ··· – energy grass (*Agropyron*); □□□ – *Miscanthus sinensis* (Chinese silvergrass)

The *m*/*z* 84 ion (Fig. 2e) corresponds to furanone, whereas the *m*/*z* 96 ion (Fig. 2f) represents furaldehyde. Furanone is released during cellulose decomposition, and furaldehyde is formed from both cellulose and hemicellulose. The *MS* sample gives only one *m*/*z* 96 peak in agreement with the previous results: the shoulder before the main peak corresponding to hemicellulose decomposition is not as well-discernible as for the other samples.

The thermal decomposition of the samples has also been investigated in the presence of oxygen in order to get some insight into the role of oxygen and into the burn-off of the char. Figure 3a shows the TG and DTG curves of the samples. The main DTG peak corresponds to the devolatilization process. The smaller peak above 360–400°C can be attributed to the burn-off of the previously formed char. The DTG curves of the herbaceous species are found at a lower temperature than those of the wood species. The rate of decomposition ($DTG_{max}$) is considerably higher for the wood samples than for the grasses. Figure 3a also confirms that the decomposition of cellulose and hemicellulose are better separated in the case of the wood species as the distinct shoulders on the main DTG peak imply. The burn-off of the char proceeds in the 360–460°C temperature range. The height of these small peaks is related to the amount of char formed in inert atmosphere (Fig. 1).

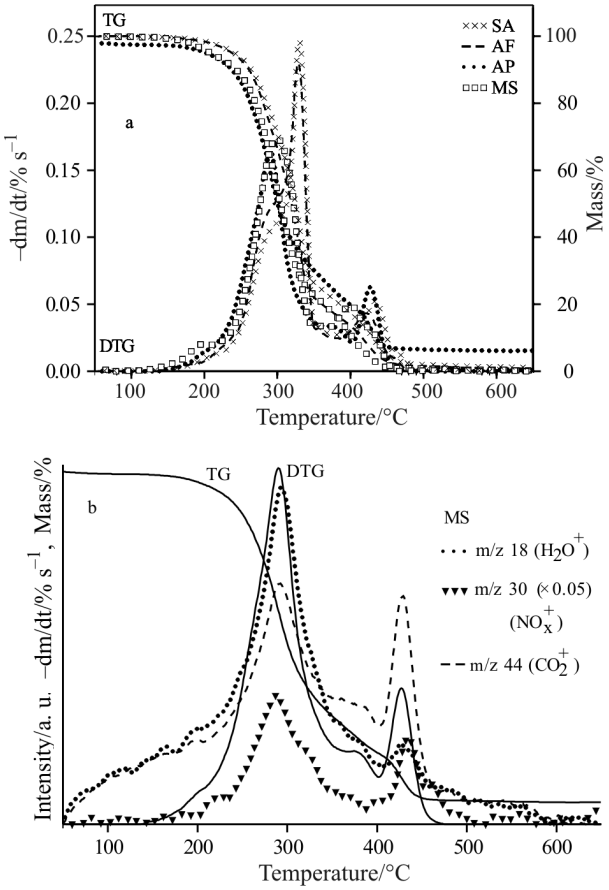


**Fig. 3** a – TG, DTG curves of the samples and b – MS curves of *Miscanthus sinensis* in oxidative atmosphere

The most important products of decomposition in oxidative atmosphere are water (*m*/*z* 18) and carbon dioxide (*m*/*z* 44) as Fig. 3b shows. (Note that in this figure the MS curves of the *Miscanthus sinensis* sample are shown as examples. Nevertheless, the decomposition products are similar for all studied samples.) Besides these gases the formation of a smaller amount of *m*/*z* 30 was detected, which indicates the formation of nitrogen oxides ($NO_x$).

*Results of the PCA calculation*

Principal component analysis has been used to compare the samples and to find correlations between the data. In the first step the thermogravimetric characteristics of the samples (determined in inert and oxidative atmospheres as described previously [6, 20]) and the data of Table 1 have been used as input data. In this calculation the first principal component described 71.2% of the total variance of the data, and the second principal component accounted for 20.1% of the variance. In the second step the integrated intensities of the fragment ions listed in Table 2 have been used in the chemometric evaluation. In this case 64.4 and 26.9% of the total variance was explained by the first and second principal components, respectively. Figure 4 depicts the results of the PCA calculations. The thermogravimetric characteristics of the energy grass sample (*AP*) (Fig. 4a) clearly differ from the other samples as the distance of the *AP* sample from the other samples implies. The wood samples are distinguished from the herbaceous samples on the first principal component domain, however, they are farther away from one another than one would expect from the rather similar TG and DTG curves (Figs 1 and 3). The corresponding loading plot (Fig. 4c) suggests that the first principal component is determined by some of the thermogravimetric characteristics (mainly $T_{cell.off(ox)}$, $T_{cell.off(in)}$, etc.), the calorific value and the ash content of the samples. This figure also shows that although the char yield and the ash content are both important in determining the first component, they are not completely correlated. The temperature of the DTG peak in inert atmosphere ($T_{max(in)}$) and the amount of Klason lignin contribute mostly to the second component.

The score plot obtained in the evaluation of mass spectrometric data (Fig. 4b) also shows that the wood samples clearly constitute a separate group apart from the herbaceous species. The woody and herbaceous biomass samples are separated along the second prin-

**Table 2** List of the most important fragment ions detected with the mass spectrometer during the decomposition of biomass samples and the origin of the fragment ions (Note that only fragment ions with good signal:noise ratio are listed, which were used in the PCA calculation)

| *m*/*z* | Fragment ion | Origin* |
|---|---|---|
| 2 | $H_2^+$ | charring processes |
| 16 | $CH_4^+$ | decomposition of polymers |
| 18 | $H_2O^+$ | decomposition of polymers |
| 27 | $C_2H_3^+$ | decomposition of polymers, decomposition of extractive compounds |
| 28 | $CO^+$ | decomposition of polymers |
| 29 | $CHO^+$ | decomposition of polymers |
| 30 | $HCHO^+$ | decomposition of polymers |
| 31 | $CH_3O^+$ | decomposition of polymers, scission of lignin sidegroups |
| 43 | $CH_3CO^+$ | decomposition of polymers |
| 44 | $CO_2^+$ | decomposition of polymers |
| 45 | $COOH^+$ | decomposition of polysaccharides |
| 55 | $C_4H_7^+$ | decomposition of polymers, decomposition of extractive compounds |
| 58 | $CH_3COCH_3^+$ | decomposition of polysaccharides |
| 60 | $HOCH_2CHO^+$+$CH_3COOH^+$ | decomposition of polysaccharides |
| 74 | $C_3H_6O_2^+$ (hydroxypropanal) | decomposition of polysaccharides |
| 82 | $C_5H_6O^+$ (2-methylfuran) | decomposition of polysaccharides |
| 84 | $C_4H_4O_2^+$ (furanone) | decomposition of cellulose |
| 96 | $C_5H_4O_2^+$ (2-furaldehyde) | decomposition of polysaccharides |
| 98 | $C_5H_6O_2^+$ (dihydro-methylfuranone) | decomposition of polysaccharides |

*Decomposition of polymers refers to the decomposition of all cell-wall constituting polymers (cellulose, hemicellulose and lignin).

cipal component. The loading plot (Fig. 4d) shows the original variables (integrated intensities of the different *m*/*z* fragment ions) in the field of the principal components. The *m*/*z* 2 and 16 ions and some oxygen containing fragments and decomposition products (*m*/*z* 29, 31, 43, 45, 82, 84, 98) account mostly for the first principal component. The *m*/*z* 27, 28 and 44 ions play the most significant role in determining the second principal component.

Figures 4b and d also imply what the most important differences between the samples are. The charring processes indicated by the evolution of $H_2$ (*m*/*z* 2) and $CH_4$ (*m*/*z* 16) are the most pronounced in the case of the energy grass sample (*AP*), which has the highest char and ash content. It can also be seen

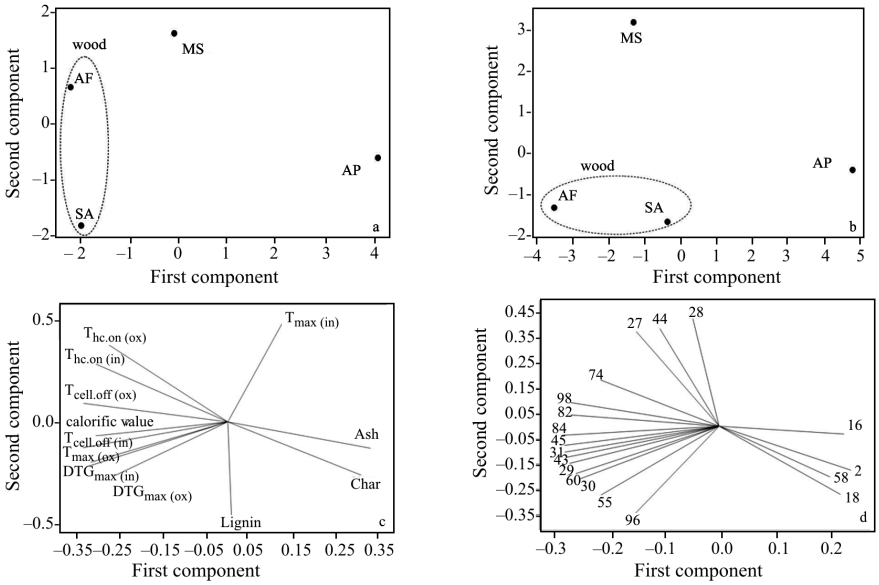


**Fig. 4** Results of the principal component analysis; score plot based on a – PCA of TG and other analytical data and b – the MS intensities of selected fragment ions; loading plot based on c – PCA of TG and other analytical data and d – the MS intensities of selected fragment ions

that energy grass decomposes at the lowest temperature ($T_{max(in)}$). The largest amount of $C_2H_3^+$, $CO^+$ and $CO_2^+$ was released by the *Miscanthus sinensis* sample. These may be the decomposition products of extractive compounds, which are presumably present in this sample in a larger amount than in the other species. Note that this assumption is confirmed by the DTG and MS curves presented in Figs 1–3: a small peak can be observed before the main peak in the corresponding figures, which is not as pronounced in the case of the other samples. A larger amount of oxygen containing volatile compounds is released from the wood samples than from the herbaceous species. Nonetheless, the relative amounts of the different decomposition products are different from the two wood species reflecting the different composition of the two samples: willow (*SA*) has a larger Klason lignin content than water locust (*AF*), accordingly, the ratio of polysaccharides is smaller in the *SA* sample.

## Conclusions

Characteristic differences have been found in the thermal behavior of the four studied biomass samples. The wood samples exhibited some similarities: the temperature range of decomposition, the shapes of the DTG curves and the evolution profiles of different products were similar. The most significant difference between willow and water locust was observed in the range of hemicellulose decomposition: the heights of the corresponding DTG and MS peaks were smaller for the willow sample. On the other hand, the char yield and lignin content of willow was higher. The behavior of the herbaceous samples exhibits more significant differences. The shapes of the DTG and MS curves of *Miscanthus sinensis* and energy grass were different implying a considerably different composition of these species. The thermal characteristics of the *Miscanthus sinensis* sample were more similar to those of the wood samples than those of the energy grass.

Principal component analysis offered a simple and reliable way to compare the samples. The loading plots gave insight into the underlying differences between the samples, and correlations of the original variables could be determined with their help.

## Acknowledgements

This work was supported by the Hungarian National Research Fund (OTKA K61504 and T037705). The authors thank Professor Béla Marosvölgyi for providing the samples. The authors are also grateful to the Agency for Research Fund Management and Research Exploitation for its financial support.

## References

1 A. Demirbaş, Energy Convers. Manage., 42 (2001) 1357.
2 A. V. Bridgwater in A. V. Bridgwater, Ed., Thermochemical Processing of Biomass, Butterworths, London 1984, pp. 35–52.
3 P. Szabó, G. Várhegyi, F. Till and O. Faix, J. Anal. Appl. Pyrol., 36 (1996) 179.
4 L. Nunez-Reguiera, J. A. Rodriguez-Anon, J. Proupin, B. Mourino and R. Artiaga-Diaz, J. Therm. Anal. Cal., 80 (2005) 457.
5 C. Erlich, E. Bjornbom, D. Bolado, M. Giner and T. H. Fransson, Fuel, 85 (2006) 1535.
6 M. G. Grønli, G. Várhegyi and C. DiBlasi, Ind. Eng. Chem. Res., 41 (2002) 4201.
7 J. Kaloustian, A. M. Pauli and J. Pastor, J. Therm. Anal. Cal., 53 (1998) 57.
8 Å. Ingemarsson, M. Nilsson, J. R. Pedersen and J. O. Olsson, Chemosphere, 39 (1999) 103.
9 K. Senelwa and R. E. H. Sims, Biomass Bioenerg., 17 (1999) 127.
10 I. Laureysens, W. Deraedt, T. Indeherberge and R. Ceulemans, Biomass Bioenerg., 24 (2003) 81.
11 E. Mészáros, E. Jakab, G. Várhegyi, P. Szepesváry and B. Marosvölgyi, J. Anal. Appl. Pyrol., 72 (2004) 317.
12 G. Skodras, O. P. Grammelis, P. Balinas, E. Karakas and G. Sakellaropoulos, Ind. Eng. Chem. Res., 45 (2006) 3791.
13 G. Várhegyi, E. Jakab, F. Till and T. Székely, Energ. Fuel, 3 (1989) 755.
14 M. Wesołowski and P. Konieczyński, Thermochim. Acta, 397 (2003) 171.
15 T. Adam, T. Ferge, S. Mitschke, T. Streibel, R. R. Baker and R. Zimmermann, Anal. Bioanal. Chem., 381 (2005) 487.
16 H. Yokoi, T. Nakase, Y. Ishida, H. Ohtani, S. Tsuge, T. Sonoda and T. Ona, J. Anal. Appl. Pyrolysis, 57 (2001) 145.
17 S. Kokot and P. Yang, Anal. Chim. Acta, 304 (1995) 297.
18 M. Statheropoulos, K. Mikedi, N. Tzamtzis and A. Pappa, Anal. Chim. Acta, 461 (2002) 215.
19 M. Statheropoulos and K. Mikedi, Anal. Chim. Acta, 446 (2001) 353.
20 E. Mészáros, G. Várhegyi, E. Jakab and B. Marosvölgyi, Energ. Fuel, 18 (2004) 497.
21 R. Kataki and D. Konwer, Biomass Bioenerg., 20 (2001) 17.
22 H. Hafizoglu, M. Usta and Ö. Bilgin, Holzforschung, 51 (1997) 114.

DOI: 10.1007/s10973-006-8102-4